Improving Frequency Stability Based on Distributed Control of Multiple Load Aggregators

Hu, Jianqiang; Cao, Jinde; Guerrero, Josep M.; Yong, Taiyou; Yu, Jie

Published in:
I E E E Transactions on Smart Grid

DOI (link to publication from Publisher):
10.1109/TSG.2015.2491340

Publication date:
2017

Document Version
Early version, also known as pre-print

Improving Frequency Stability Based on Distributed Control of Multiple Load Aggregators

Jianqiang Hu, Jinde Cao, *Senior Member, IEEE*, Josep M. Guerrero, *Fellow, IEEE*, Taiyou Yong, *Senior Member, IEEE*, Jie Yu, *Member, IEEE*

***Abstract*—In the power demand side, responsive loads can provide fast regulation and ancillary services as reserve capacities in interconnected power systems. This paper presents a distributed pinning demand side control (DSC) strategy for coordinating multiple load aggregators, i.e., aggregated responsive loads, to provide frequency regulation services. Specifically, a leader-following communication protocol is considered for the load aggregators, in which there is a centralized pinner (leader) and multiple load aggregators (followers). The regulation objective is generated from the pinner and only shared with a small fraction of load aggregators. Moreover, a multi-step algorithm is proposed to determine the control gains in the DSC, which not only guarantees the stability of the close-loop system, but also restrains the plant disturbance. Furthermore, the distributed pinning DSC algorithm is integrated into the traditional centralized PI-based AGC framework, which has formed the coupled secondary frequency control structure. It has been shown that the total power mismatch in each control area is shared with both AGC units and load aggregators and the system frequency can be improved by considering the distributed pinning DSC for load aggregators. Finally, simulation results are provided to demonstrate the effectiveness of the proposed coupled frequency control strategy.**

***Index Terms*—Frequency regulation, demand side control, load aggregator, Distributed control, Pinning consensus.**

NOMENCLATURE

M	Number of control areas in the power system
N_i	Number of load aggregators in ith control area
ni	Number of generating units in ith control area
Δf_i	Frequency deviation from the normal value in ith control area
ΔP_{Li}	Mismatched active power in ith control area
ΔP^{+}_{max}	Upper regulation capacity of AGC units in the current control area
ΔP^{-}_{min}	Lower regulation capacity of AGC units in the current control area
$\Delta P_{tie,i}$	Tie-line power deviation in ith control area
ΔP_{Ci}	Control action for AGC units in ith control area
T_{ij}	Synchronizing coefficient with jth control area
D_i	Area load frequency characteristic in ith control area
H_i	Area equivalent inertia in ith control area
R_i	Speed droop characteristic in ith control area
B_i	Frequency bias coefficient in ith control area
α	Participation factor for AGC units in ith control area
$P^{L}_{j,*}$	Optimal operational power for jth load aggregator
$P^{L}_{j,max}$	Maximal regulation capacity of jth load aggregator
γ	$H\infty$ control preferment index
κ	Positive feedback gain of the centralized pinner in the DSC
β	Coupling strength of the distributed pinning protocol
θ	Sharing proportion of AGC capacity in the current control area
$\mu_0(t)$	Utilization level of the centralized pinner
$\mu_j(t)$	Utilization level of jth load aggregator
$u_j(t)$	Communication protocol of jth load aggregator
$y_j(t)$	Measured actual power output for jth load aggregator
AGC	Automatic generation control
DSC	Demand side control
ACE	Area control error

Manuscript received March 13, 2015; revised July 06, 2015, and August 13, 2015; accepted October 11, 2015.

This work was jointly supported in part by the State Grid Corporation of China under Project DZ71-13-045: Study on Key Technologies for Power and Frequency Control of System with "Source-Grid-Load" Interactions, in part by the National Natural Science Foundation of China under Grant nos. 61573096 and 61272530, and the 333 Engineering Foundation of Jiangsu Province of China under Grant no. BRA2015286, in part by the Fundamental Research Funds for the Central Universities, in part by the JSPS-China Innovation Program under Grant KYLX_0135, and in part by the Scientific Research Foundation of Graduate School of Southeast University under Grant YBJJ1448.

J. Hu is with School of Automation and Key Laboratory of Measurement and Control of CSE, Ministry of Education, Southeast University, Nanjing 210096, China. E-mail: jqhuseu@gmail.com.

J. Cao is with Research Center for Complex Systems and Network Sciences, and Department of Mathematics, Southeast University, Nanjing 210096, China, and also with Department of Mathematics, Faculty of Science, King Abdulaziz University, Jeddah 21589, Saudi Arabia. E-mail: jdcao@seu.edu.cn.

J. M. Guerrero is with the Department of Energy Technology, Aalborg University, Aalborg DK-9220, Denmark. E-mail: joz@et.aau.dk.

T. Yong is with China Electric Power Research Institute, Nanjing 210003, China. E-mail: yongtaiyou@epri.sgcc.com.cn.

J. Yu is with School of Electrical Engineering, Southeast University, Nanjing 210096, China. E-mail: friendlyyu2000@aliyun.com.

I. INTRODUCTION

Frequency stability and control are essential for the safe operation of power systems, which are closely related to the balance of active power between generation and consumption. With the development of smart grids and energy networks, power systems are facing a high penetration of renewable generations and smart loads (towards future power systems), which may result in difficulties in frequency control [1]. Generally, generating and reserve units need to follow the load fluctuation so as to maintain the frequency within specified limits. This load following process takes place in three, timely decoupled stages, which form three distinct frequency control levels in power systems [2].

Primary frequency control exists on the first regulation process, which is a decentralized proportional control (i.e.,

droop control) designed to stabilize the frequency following large generation or load outages. All the generators are equipped with droop controllers to drive the speed governor to perform this control automatically. *Secondary frequency control* is a centralized automatic control that adjusts the active power output of the generating units to restore the frequency and the interchanges with other control areas to their target values following an imbalance. While, only partial generators are equipped with secondary frequency controllers and the capacity of these AGC units is always limited. Moreover, external spinning reserves must be available in the system to compensate for the shortage of regulation capacity for this part. *Tertiary frequency control* refers to the unit commitment and economic dispatch of generating units, which aims at redistributing the load to generating units economically. For the secondary and tertiary control, they are often realized within different control areas [3]. The response time of these control levels varies from seconds to days. The primary frequency control reacts very quickly within the first few seconds after a disturbance; AGC responds in a time interval from 10 s to 5 min and spinning reserves can be activated in 5 min to 15 min. Tertiary reserves (operating reserves and capacity reserves) are manually activated after the secondary reserves [4].

In future power systems, the above mentioned three control levels may not regulate the system frequency in a satisfactory way for a decreasing trend of the rotational inertia in the system. This rotational inertial is crucial in restricting the rate of change of frequency (ROCOF) right after the occurrence of a power contingency [5]. Therefore, extra frequency reserve provisions are needed to supply timely services in power systems with high penetration.

Demand side resources have considerable potential, which can provide efficient ancillary services (regulation, spinning reserve, and operating reserve) so as to maintain the supply-demand balance together with traditional generating units [6], [7]. For instance, demand side reserves are integrated into unit commitment problems, which could reduce the generation cost and improve the number of maximum possible multiple contingencies [8]. Demand response problem of China has been discussed in [9], which still has broad space to be implemented. The focus of these demand response services has generally been on responsive loads, such as water heaters, air conditioners, heat pumps, refrigerators, and electric vehicles. They could change their consumption levels by detecting the system frequency or responding to the time-based energy price signal (known as indirect load control), or executing load curtailment or load shedding actions (known as incentive-based direct load control), according to Federal Energy and Regulatory Commission (FERC), for more details, see [10], [11].

Compared with the number of generating units, the number of responsive loads is pretty copious. Meanwhile, the distribution of these loads is decentralized in different control areas [12]. Generally, responsive loads are aggregated to numerous load aggregators, by which groups of loads can emerge the desired characteristic like generation. Such an aggregation process is beneficial, because markets typically require that participating resources must have a minimum capacity which is well beyond each single load [13]. Load aggregator, which can also be viewed as a load utility, is composed of abundant terminal loads, such as, electric vehicle (EV) aggregator, thermostatically controlled load (TCL) aggregator. The objective of a load aggregator is to regulate the total load consumption so as to track the scheduled electricity profile, which serves as an interface between users and the grid operator with joint consideration for benefits of both users and the grid. Even so, the number of load aggregators is considerable. How to control these load aggregators becomes a critical problem.

Frequency regulation contributed from the demand side resources is always implemented in two general classes of control modes: centralized and decentralized strategies. Centralized control is closed related to a secure star communication network, which can present a high degree of controllability and reliability. According to a centralized reserve provision algorithm, demand response resources were cooperated with spinning reserves for balancing generation and demand in [14] under power contingency conditions. Based on a centralized hierarchical model predictive control algorithm [3], electric vehicles were integrated into the smart grid to provide frequency regulation service together with generating units. The authors in [15] considered the centralized load control problem for a large population of thermostatically controlled appliances (TCAs) and shown that they could provide the regulation and load following services.

While, decentralized control does not depend on explicit communications, each terminal load makes a decision based on a local measurement unit. For example, by proposing a dynamic frequency threshold control and incorporating it into certain consumer appliances [16], it had been indicated that this control strategy could improve the frequency stability and reduce the dependence on rapidly deployable backup generation. The authors in [17] shown that the aggregated responsive load was close to a synchronous generator when participating in frequency control based on decentralized frequency deviation signals. In Ref. [18], decentralized optimal load control problem was considered based on local frequency measurement and neighborhood area communication, which could serve as a contingency reserve for the power system.

Traditional centralized management strategy perceived difficulties in dealing with abundant terminal responsive loads rather than a limited number of generating units. For example, millions of terminal load devices connected in a 16-layer deep wireless meshed network often result in unaccepted stochastic delay for critical applications if the control signal is issued from the control center [7]. Some responsive loads supplying regulation must be capable of receiving control signals every 6 seconds, which will pose significant challenges for communication [19]. While for the decentralized control, collective behavior of all terminal loads will be definitely interesting and worth noting. On the other hand, certain complexities might arise from local measurement units, such as, local measurement of power frequency signal with proper precision is a hard task in demand response management systems.

Recently, distributed control, as the third control strategy (centralized, decentralized and distributed), has received considerable attention in scenarios of multiple interactive units in

power systems. For example, a distributed multi-agent-based load shedding algorithm was proposed in [20], which could make efficient load shedding decision when the generation was insufficient to power all loads. Distributed control was utilized to coordinate multiple energy storage units (ESUs) [21] and it was shown that such a control strategy could improve the control capability in the regulation of frequency and voltage. The authors in [22] proposed a distributed frequency regulation framework to coordinate multiple prosumers (proudcer-consumer) in electric energy systems. Average consensus algorithm was utilized in [23] to distribute portions of the desired aggregated demand among multiple residential energy management systems. In Ref. [24], distributed secondary control for islanded microgrids was discussed based on a distributed networked control system.

In the present paper, a novel distributed pinning control for coordinating multiple load aggregators is proposed such that active power compensation contributed from load aggregators takes place at the secondary frequency control process to assist AGC units in restoring frequency stability when a large power mismatch occurs. Different from previous literatures, we consider a leader-following communication structure for multiple aggregated responsive loads, in which there are a central pinner unit and multiple following units. The regulation objective generated from the pinner is only shared with a small fractional of load aggregators instead of issuing to all ones (if issued, i.e., centralized control), and the remaining load aggregators coordinate each other to achieve the scheduled regulation objective through a dispersed communication. It has been demonstrated that the frequency stability can be improved considerably by integrating the DSC of multiple load aggregators to the traditional AGC framework.

To summarize, the main contributions of this paper are listed as follows: (1) A distributed pinning DSC strategy for coordinating multiple load aggregators has been proposed, which is better than the traditional centralized or decentralized control in terms of robustness and scalability; (2) DSC algorithm has been integrated into the secondary frequency control structure to provide ancillary services with generating side AGC units; (3) Stability about the proposed DSC algorithm against the plant disturbance is provided and a multi-step algorithm is given to determine the control gains in the DSC algorithm.

The rest of the paper is organized as follows. In Section II, problem formulation and some preliminaries on frequency regulation model with DR resources are briefly outlined. In Section III, the distributed pinning DSC for multiple load aggregators is designed and the feedback control gains are determined by a two-step algorithm. Case studies are provided in Section IV to demonstrate the effectiveness of the proposed coupled frequency control strategy. Finally, discussions are provided in Section V and conclusions are drawn in Section VI.

II. Problem Formulation and Some Preliminaries

A. Problem formulation

Suppose that the power system is working around an operating point where the total load demand and the total generation are not balanced. All load aggregators in each control area are managed by a load agent. Load agents and power plants can obtain their regulation capacities through bidding in a regulation market or from system operator in a deregulated system. The mismatched power in each control area can be calculated form ACE signal in the transient process. Furthermore, based on the ACE signal, we consider the detailed active power allocation strategy for AGC units and multiple load aggregators in each control area. Note that the traditional centralized control strategy is still utilized for AGC units. While, for the load aggregators, we propose a novel distributed pinning control strategy.

Taking a single-control area power system for an example, assuming the mismatch of active power between the total demand and the overall power generated is ΔP_L. For the multiple load aggregators in the control area, they are distributed over a communication network. Suppose the communication network of the load aggregators is modelled by a digraph $\mathcal{G} = \{\mathcal{V}, \mathcal{E}, A\}$, where the nodes $\mathcal{V} = \{1, 2, \ldots, N\}$ in the network denote the set of load aggregators and the links $\mathcal{E}$ denote the set of communication links. The edge $e_{ij} = (i, j) \in \mathcal{E}$ indicates that the jth aggregator can receive the information from the ith aggregator. A graph is said to be undirected if $e_{ij} \in \mathcal{E}$ implies $e_{ji} \in \mathcal{E}$. A directed tree is a digraph, where every node, except the root, has exactly one parent node. A spanning tree of $\mathcal{G}$ is a directed tree whose node set is $\mathcal{V}$ and whose edge set is a subset of $\mathcal{E}$. For a digraph $\mathcal{G}$, the adjacency matrix $A \in \mathbb{R}^{N\times N}$ is defined as $a_{ij} \geq 0$, in which $a_{ij} = 1 \Leftrightarrow e_{ji} = (j, i) \in \mathcal{E}$ while $a_{ij} = 0$ if $e_{ji} \notin \mathcal{E}$, and it is further required that self links are not allowed, *i.e.*, $a_{ii} = 0$. The Laplacian matrix L is defined as $L = \mathcal{D} - A$, where $\mathcal{D}$ is a diagonal matrix with $\tilde{d}_{ii} = \sum_{j\neq i} a_{ij}$.

The objective of the distributed coordination of the load aggregators is to drive the mismatch ΔP_L towards the regulation interval $(\Delta P^-_{min}, \Delta P^+_{max})$ of online AGC units. That is, how to share the mismatched power with both AGC units and load aggregators by considering the regulation capacity limit of AGC units. Such a coupled control structure is presented in Fig. 1, in which generating control and demand side control coexisted.

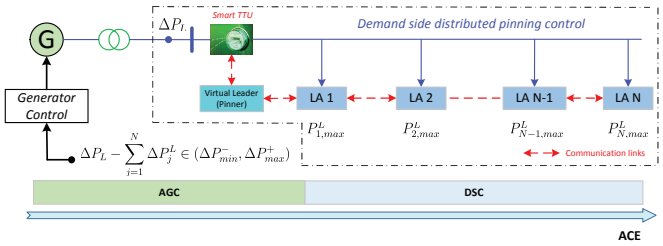

Fig. 1. Coupled active power allocation structure of power systems in a control area.

In the proposed distributed pinning control strategy, there is a virtual leader (also called the centralized pinner), which is utilized to generate a virtual pinning regulation signal for all load aggregators. This pinning signal is only shared with a small fractional of load aggregators (called followers in the distributed pinning system) and other load aggregators

communicate with their neighbors. Such a distributed pinning strategy can realize the fair participation for all load aggregators. On the other hand, the coordination of these load aggregators can fulfill an expected regulation objective.

The reason why we utilize a distributed pinning strategy is at least in three aspects: (1) Compared with limited numbers of AGC units, the number of load aggregators is large and the distribution of these load aggregators is decentralized in a wide range of areas, which resulted the traditional centralized allocation strategy is time-consuming and inefficient. (2) Load aggregators have more flexibility, they can choose to participate the DR or not by their own hobby, where distributed strategy can provide a more robust solution to handle with this scenario and realize the plug-in and plug-out of load aggregators. (3) Different from the classical distributed average consensus strategy, there is a global coordination objective to fulfill the expected active power regulation in this problem. So, the distributed pinning strategy (i.e., leader-following strategy) is the optimal allocation strategy for the management of numerous load aggregators.

B. Implementing frequency regulation from AGC+DSC

Aggregated responsive loads, similar to negative generating units, can also be utilized to provide the primary and secondary frequency regulation services. Instead of generating units with physical constraints, these responsive loads can fulfill the demand in a faster time scale and are capable of ramping up or down faster than the traditional generators. In this subsection, we will focus on the provision of secondary frequency control from aggregated responsive loads by supporting the existing AGC service in the power system. Suppose there are M control area in the interconnected power system, and the frequency regulation system with aggregated responsive loads of ith control area is provided in Fig. 2. It is easy to derive the system frequency model as follows.

$$\begin{aligned}\Delta f_i(s) =&\frac{1}{2H_i s + D_i}\Big\{\sum_{j=1}^{N_i}\Delta P_{ji}^L(s) - \Delta P_{Li}(s)\\ &+\sum_{k=1}^{n} M_{ki}(s)\big[\Delta P_{Cki}(s) - \frac{1}{R_{ki}}\Delta f_i(s)\big]\\ &-\Delta P_{\text{tie},i}(s)\Big\},\end{aligned}$$

where the dynamic of turbine-governor is

$$M_{ki}(s) = \frac{1}{(1+T_{gk}s)}\cdot\frac{1}{(1+T_{tk}s)},$$

and the tie-line power deviation is

$$\Delta P_{\text{tie},i}(s) = \frac{2\pi}{s}\Big[\sum_{j=1,j\neq i}^{M} T_{ij}(\Delta f_i - \Delta f_j)\Big],$$

where T_{gk} and T_{tk} are governor and turbine time instants, respectively.

The state-space model of LFC (load frequency control) dynamical system with DR participation in ith control area can be obtained as follows

$$\begin{cases}\dot{x}_i = A_i x_i + B_{1i}\Delta P_{Li} + \sum_{j=1,j\neq i}^{N} T_{ij}\Gamma x_j\\ \qquad\quad + B_{2i}\Delta P_{Ci},\\ y_i = C_{yi}x_i, \qquad i = 1,2,\ldots,M,\end{cases} \tag{1}$$

where the state $x_i = [\Delta f_i, \Delta P_{\text{tie},i}, x_{mi}, x_{gi}]^T \in \mathbb{R}^{2ni+2}$, the output $y_i = ACE_i = B_i\Delta f_i + \Delta P_{\text{tie},i} \in \mathbb{R}$. Furthermore, the internal states x_{mi} and x_{gi} are refined to $x_{mi} = [\Delta P_{m_{1i}}, \ldots, \Delta P_{m_{ni}}]$ and $x_{gi} = [\Delta P_{g_{1i}}, \ldots, \Delta P_{g_{ni}}]$. The control input $\Delta P_{Ci} = f(ACE_i) - \sum_{j=1}^{N_i}\Delta P_{ji}^L$. If PI control is utilized in the secondary frequency regulation, then $f(ACE_i) = k_{Pi}ACE_i + k_{Ii}\int ACE_i$, where k_{Pi} and k_{Ii} are real constant numbers. The coefficient matrices $A_i, B_{1i}, B_{2i}, C_{yi}$ and the synchronizing torque matrix $T = (T_{ij}) \in \mathbb{R}^{N\times N}$ and the inner coupling matrix $\Gamma \in \mathbb{R}^{(2ni+2)\times(2ni+2)}$ can be found in any LFC literature, thus omitted here.

In steady state, the total power mismatch is compensated by both the AGC units and the load aggregators, i.e., at the new equilibrium,

$$\Delta P_{Li} = \sum_{k=1}^{ni}\Delta P_{C_{ki}} + \sum_{j=1}^{N_i}\Delta P_{ji}^L.$$

In the presented secondary frequency regulation system, generating units are controlled by the traditional centralized control and aggregated responsive loads are controlled by the proposed distributed pinning control. The power mismatch is allocated to AGC units by the participation factors and to load aggregators by the pinning regulator, i.e., the centralized pinner. Utilizing the load aggregators to support AGC units means the control effort is shared with both the AGC units and load aggregators. The participation of responsive loads can relieve a part of AGC burden on the traditional power plants and improve the frequency stability of the power system.

III. Distributed Pinning Control of Multiple Load Aggregators

In this section, we provide the detailed designing algorithm for multiple load aggregators in one control area. The control objective is to achieve the fair participation for all load aggregators proportional to its maximum regulation capacity (i.e., the utilization level). A centralized pinner is introduced to generate a virtual iterative signal (i.e., pinning utilization level), which can guide the whole group moving towards the global objective asymptotically. The centralized pinner can be viewed as a dynamic high level control structure, which is only connected to a small fraction of load aggregators and the communication network of these load aggregators is described by a digraph.

To achieve the fair participation for all the load aggregators, the required active power is to be shared at the same ratio as its maximum available active power regulation capacity for each load aggregator ($P_{j,max}^L$). Suppose the active power of jth load aggregator under the current environment is $P_j^L(t)$, then the fair regulation issue among multiple load aggregators means

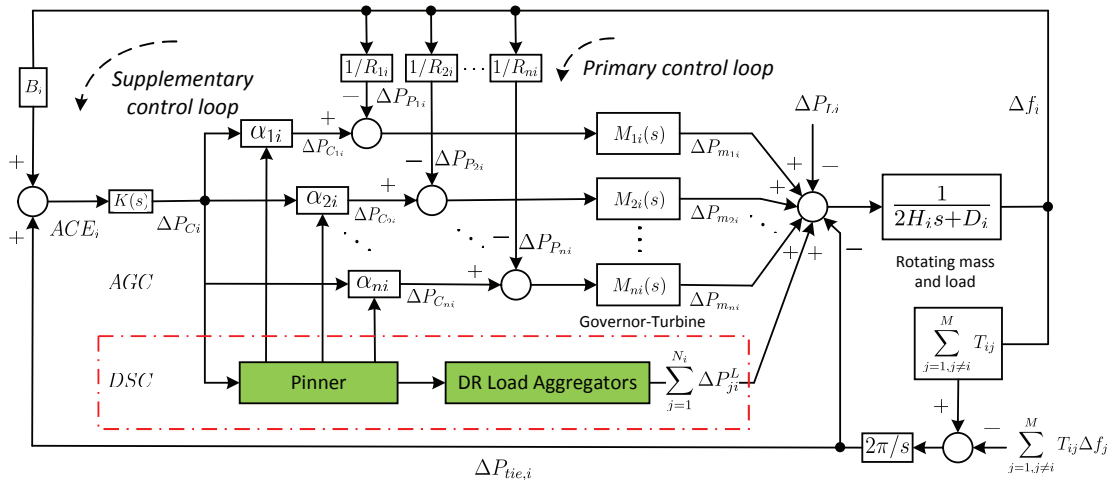

Fig. 2. System frequency response model with demand side control of flexible load aggregators.

that each aggregator should operate at an identical ratio, i.e., pinning consensus participation. So, at the equilibrium, there is:

$$\frac{P_1^L}{P_{1,max}^L} = \frac{P_2^L}{P_{2,max}^L} = \cdots \frac{P_N^L}{P_{N,max}^L} = \mu^*, \tag{2}$$

where μ^* is the steady state pinning equilibrium.

The pinner is updated by a first-order differential equation, in which the right side is related to the total mismatched power in the current control area, iteration results of all load aggregators, and the active power regulation capacity of online AGC units. The internal control structure of the leader is shown in Fig. 3.

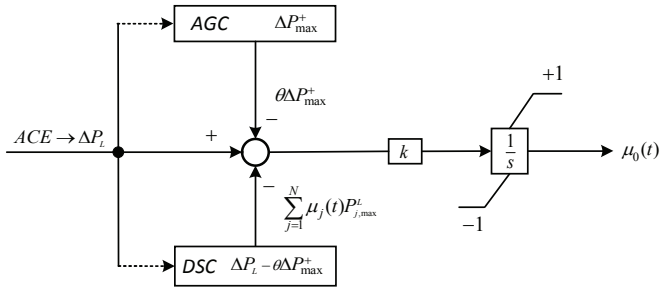

Fig. 3. Control structure for the centralized pinner (3).

The mismatched power is shared with both AGC units and load aggregators in this control area. And these two kinds of participants can be involved in the energy markets to gain the regulation capacities through dynamic bidding, respectively. Thus, the sharing proportion θ of AGC capacity can be determined easily. Here, we consider the scenario of a positive power mismatch, i.e., $\Delta P_L > 0$. The pinner initiates the pinning rate μ_0 by

$$\dot{\mu}_0(t) = \kappa\Big(\Delta P_L - \theta\Delta P_{max}^+ - \sum_{j=1}^{N} \mu_j(t) P_{j,max}^L\Big) \tag{3}$$

with the initial value $\mu_0(0) = 0$, where μ_0 is the state of the virtual leader, κ is a positive feedback gain to be determined, and the coefficient θ is a positive constant satisfying $0 \le \theta \le 1$; $\mu_j(t)$, $j = 1, 2, \ldots, N$ are the utilization levels for the load aggregators. Thus, $\sum_{j=1}^{N} \mu_j(t) P_{j,max}^L$ is the total amount of power regulation of all aggregated responsive loads at the sampling time t, which can be detected by the transformer terminal unit (TTU) installed at the terminal of the load agent. For the leader (3), it is easy to derive that the equilibrium μ^* satisfies the following equation:

$$\Delta P_L - \theta\Delta P_{max}^+ - \sum_{j=1}^{N} \mu^* P_{j,max}^L = 0. \tag{4}$$

Remark 1. *The coefficient θ in the leader (3) can be varied from 0 to 1 according to the economic costs of both units in the regulation market or the system operator. When $\theta = 0$, all the power mismatch is taken by responsive loads. However, it may lead to high costs for some load aggregators, such as, industrial ventilation equipment, especially when the online AGC units are capable of the regulation at a lower cost. When $\theta = 1$, the AGC units are operated at a full load. Such a case should be avoided for the operation security and economic cost of generators, meanwhile additional ancillary services are needed.*

Next, we consider the simple control model of N load aggregators. The control structure of each load aggregator is simplified by an integrator, i.e., the dynamics of jth controller installed at the terminal of jth load aggregator can be expressed by:

$$\begin{cases} \dot{\mu}_j(t) = \omega_j(t) + u_j(t), \\ y_j(t) = \mu_j(t) P_{j,max}^L, \quad j = 1, 2, \ldots, N, \end{cases} \tag{5}$$

where $\omega_j(t) \in \mathcal{L}_2[0, \infty)$ (space of square integrable functions over $[0, \infty)$) is the plant disturbance for jth load aggregator. The objective is to design the communication protocol $u_j(t)$, $j = 1, \ldots, N$ such that the utilization level of each load aggregator could track the pinning rate μ_0 of the virtual leader.

Under the influence of the plant disturbance, it may be hard for the aggregator of responsive loads to respond accurately to

the pinning rate. In view of this, we attempt to design a distributed communication protocol to attenuate the interference of the plant disturbance to the pinning consensus performance. In the following, we always assume that the total regulation capacity and reserve capacity are capable of coping with the mismatch power in this control area.

To relieve communication and information transmission burden for the load aggregators by centralized control, a distributed control strategy which utilizes the local communication with load aggregator's neighbors is a good choice. In this subsection, we consider the following distributed pinning consensus protocol, which is composed of two items with the first one being the distributed communication and the second one being the pinning selection:

$$u_j(t) = \beta \sum_{k=1}^{N} a_{jk}\big(\mu_k(t) - \mu_j(t)\big) - \beta d_j\big(\mu_j(t) - \mu_0(t)\big), \tag{6}$$

where a_{jk} is the element of the adjacent matrix A of the communication topology among the load aggregators; and $d_j = 1$ if the jth load aggregator is pinned by the virtual leader, otherwise $d_j = 0$.

By substituting the control protocol (6) back to (5) and defining the error variances $r(t) = \mu_0(t) - \mu^*$ and $e_j(t) = \mu_j(t) - \mu_0(t)$, one can further derive the corresponding error systems:

$$\begin{cases} \dot{r}(t) = -\kappa \sum_{j=1}^{N} \big(e_j(t) + r(t)\big) P^L_{j,max}, \\ \dot{e}_j(t) = \beta \sum_{k=1}^{N} a_{jk}\big(e_k(t) - e_j(t)\big) - \beta d_j e_j(t) \\ \qquad + \kappa \sum_{j=1}^{N} \big(e_j(t) + r(t)\big) P^L_{j,max} + \omega_j(t), \end{cases} \tag{7}$$

for $j = 1, \ldots, N$.

By denoting $e(t) = [e_1(t), \ldots, e_N(t)]^T \in \mathbb{R}^N$, one can further transform the error system (7) to the following matrix form:

$$\begin{cases} \dot{r}(t) = -\kappa B\big(e(t) + \mathbf{1}_N r(t)\big), \\ \dot{e}(t) = -\beta(L + D)e(t) + \kappa(\mathbf{1}_N B)e(t) \\ \qquad + \kappa(\mathbf{1}_N B \mathbf{1}_N) r(t) + \omega(t), \end{cases} \tag{8}$$

where $B = [P^L_{1,max}, \ldots, P^L_{N,max}]$ and $\mathbf{1}_N = [1, \ldots, 1]^T \in \mathbb{R}^N$; L is the Laplacian matrix of the communication topology; $D = \mathrm{diag}\{d_1, \ldots, d_N\}$ is the pinning matrix; and $\omega(t) = [\omega_1(t), \ldots, \omega_N(t)]^T \in \mathbb{R}^N$. To this end, we define a controlled output function $z(t) = [r^T(t), e^T(t)]^T$ to measure the disagreement of $\mu_i(t)$ to the pinning rate $\mu_0(t)$, $i = 1, 2, \ldots, N$. Since $z(t) = \mathbf{0}$ implies the error $e(t) \to \mathbf{0}$, the attenuating ability of the system (5) against the external disturbance can be quantitatively measured by the H_∞ norm of the closed-loop transfer function $T_{z\omega}(s)$ from the external disturbance $\omega(t)$ to the controlled output $z(t)$, which is defined by

$$\begin{aligned} \|T_{z\omega}(s)\|_\infty &= \sup_{v \in \mathbb{R}} \sigma_{\max}(T_{z\omega}(jv)) \\ &= \sup_{\mathbf{0} \neq \omega(t) \in \mathcal{L}_2[0,\infty)} \frac{\|z(t)\|_2}{\|\omega(t)\|_2}. \end{aligned} \tag{9}$$

Therefore, the objective is to design a distributed pinning consensus protocol $u_j(t)$, $j = 1, \ldots, N$ such that $\|T_{z\omega}(s)\|_\infty < \gamma$ holds for a given index $\gamma > 0$, or equivalently, the closed-loop system satisfies the dissipation inequality

$$\int_0^\infty \|z(t)\|^2 \mathrm{d}t < \gamma^2 \int_0^\infty \|\omega(t)\|^2 \mathrm{d}t, \quad \forall \omega \in \mathcal{L}_2[0, \infty).$$

In this way, pinning consensus control of the cluster of load aggregators with external disturbances is transformed into the above H_∞ control problem [25]. So, the objective is to design a distributed pinning consensus protocol (6) such that

1). The pinning consensus of system (5) under the protocol (6) is reached in the presence of $\omega(t) = 0$, that is, $\lim_{t \to \infty} (\mu_j(t) - \mu_0(t)) = 0$, $j = 1, \ldots, N$ is satisfied for any initial values $\mu_j(0)$ of each load aggregator.

2). Under the zero initial state condition and for arbitrary $\omega_j(t) \in \mathcal{L}_2[0, \infty)$, the $\mathcal{L}_2$-induced norm of System (8) from ω to z satisfies $\|z\|_2 \leq \gamma \|\omega\|_2$.

For the distributed pinning protocol (6), a pinned node can access the objective information μ_0. That is, there is a directed link from the leader to the pinned node. If the objective trajectory μ_0 is labeled as the dynamic of the node 0, then a new digraph appears. We use the union of the digraph $\mathcal{G}$ and the node $\{0\}$ ($\tilde{\mathcal{G}} \triangleq \mathcal{G} \cup \{0\}$) to denote the pinning joint communication topology. The Laplacian matrix of $\tilde{\mathcal{G}}$ is

$$\tilde{\mathcal{L}} = \begin{bmatrix} 0 & \mathbf{0}_{1 \times N} \\ -\tilde{d} & L + D \end{bmatrix},$$

in which $\tilde{d} = [d_1, d_2, \ldots, d_N]^T$ and D is the pinning matrix defined above. Before proposing the main results, we need the following lemma.

Lemma 1. *[26] The matrix $L + D$ is a nonsingular M-matrix if and only if the pinning joint communication topology $\tilde{\mathcal{G}}$ has a directed spanning tree.*

Algorithm 1. *Under the assumption that the load pinning joint communication topology has a directed spanning tree, then the feedback gains of the leader and the communication protocol can be designed as follows:*

1) *Solve the following linear matrix equation*

$$(L + D)^T \xi = \mathbf{1}_N, \tag{10}$$

to get a positive column vector $\xi = [\xi_1, \xi_2, \cdots, \xi_N]^T$. Then, set the diagonal matrix $\Theta = \mathrm{diag}\{\xi\}$.

2) *Solving the following linear matrix inequality:*

$$\tilde{\Omega} = \begin{bmatrix} 1 - \kappa B \mathbf{1}_N & \frac{1}{2}\kappa\big((\Theta \mathbf{1}_N B \mathbf{1}_N)^T - B\big) & \mathbf{0} \\ * & \Psi & \Theta \\ * & * & -\gamma^2 I_N \end{bmatrix} < 0, \tag{11}$$

to obtain two scalars $\kappa > 0$ and $\beta > 0$, where $\Psi = I_N + \kappa \Theta \mathbf{1}_N B - \beta\big(\Theta(L + D) + (L + D)^T \Theta\big)$.

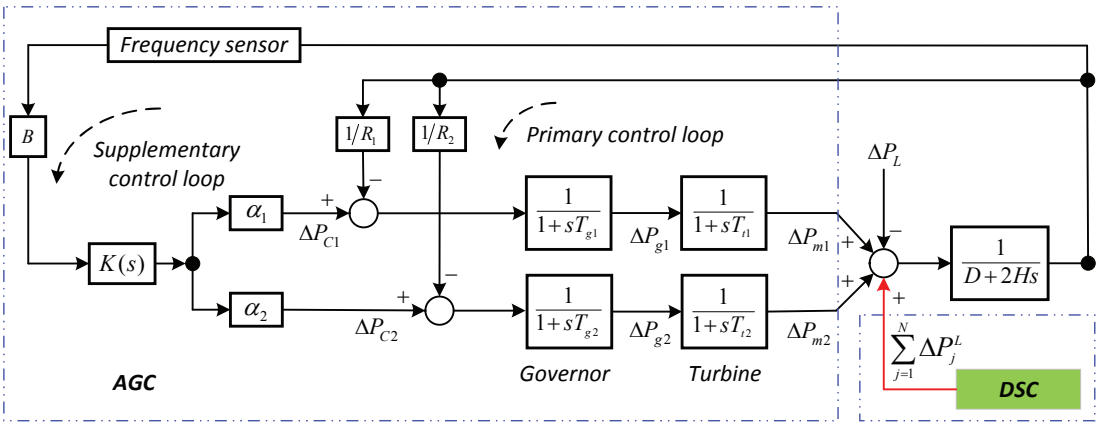

Fig. 4. The frequency control structure of single-control area power system model by considering demand side control.

Remark 2. *According to Lemma 4 in [27], the matrix Θ in step 1) is a positive definite matrix, which will be used in the step 2).*

Theorem 1. *Consider the multiple load aggregator system (5) under the assumption that the load pinning joint communication topology has a directed spanning tree, together with the distributed pinning protocol (6), if the gain parameters κ, β can be constructed by Algorithm 1, then the closed-loop error system (8) is asymptotically stable with $\|T_{\omega z}\|_2 \leq \gamma$ for a given $\gamma > 0$. That is, the load aggregator can fulfill the expected regulation objective in a fair circumstance via the proposed distributed pinning allocation strategy.*

Remark 3. *In the proposed distributed pinning communication protocol (6), a sparse communication network can be counterbalanced by a strong coupled gain; while a dense communication network can fulfill the control performance with a smaller coupled gain. In the implementation of the distributed load control, engineers can programme an optimal communication structure by setting up local communications among load aggregators, such as WiFi connections. Algorithm 1 and Theorem 1 show that the relationship between the coupled, control gains and the communication topology, pinning matrix, system parameters. On the other hand, limited transmission capacity and time delays are unavoidable in the practical communication network. Therefore, distributed pinning protocol with saturated input and communication delays need further investations, such as, utilizing saturated control input [28], determining the maximal allowable bound of delays [29] by the method of delayed networked control system [30].*

IV. Simulation Results

In this section, the proposed coupled frequency control structure is first tested on a single-control area system, and then for a three-control area scenario. The implementation of the AGC+DSC control strategy is based on Simulink in Matlab 2014a and the control performance is compared with the conventional AGC only scheme. Specifically, we formulate the simulation results from three cases, where Case 1 demonstrates the improved frequency stability in a single-control area power system; Case 2 illustrates the flexibility of the distributed pinning control strategy by plug-in or plug-out of load aggregators; Case 3 shows that the improved frequency stability in a three-control area interconnected power system.

A. Case 1: Single-control area power system

In this subsection, a single-control area power system model is employed for simulation-based experiments, where the case of two generators and one bus load agent is considered. When the power system is exposed to a large active power mismatch, additional spinning reserves are needed if the AGC units cannot undertake such a disturbance due to the operational limitations. However, multiple aggregated responsive loads under this bus load agent could provide frequency regulation services. They could be encouraged to reduce the consumption of active power by the proposed distributed pinning control in the demand side.

The frequency-based control structure of the single-control area power system with DSC is given is Fig. 4. The balance between the generation and load is achieved by detecting the system frequency to generate the primary and supplementary control signals for generators and pinner in the DSC. As for the supplementary control for the generator, we utilize the centralized PI control $K(s) = k_P \Delta f(s) + k_I \int \Delta f(s)$; and as for the load control, we utilize the proposed distributed protocol given in (6) to regulate the power consumption of multiple load aggregators. The parameters for the simulation under study are given in Tab. I.

TABLE I
Parameters used for the frequency response model.

Gen.	Rating(MW)	α_i	R_i(Hz/pu)	T_{gi}(s)	T_{ti}(s)
G1	800	0.50	2.40	0.06	0.36
G2	1000	0.50	3.30	0.07	0.42
Sys.	D(pu/Hz)	$2H$(pu s)	B(pu/Hz)	$K(s)(/s)$	
Val.	0.0084	0.1667	0.8675	$-0.2695 - 0.3788$	

According to the control structure given in Fig. 4, one can derive the following power system model with demand side contribution and without tie-line power.

$$\begin{cases} \Delta\dot{f} = -\frac{D}{2H}\Delta f + \frac{1}{2H}\left(\sum_{i=1}^{2}\Delta P_{mi} + \sum_{j=1}^{N}\Delta P_j^L - \Delta P_L\right) \\ \Delta\dot{P}_{mi} = -\frac{1}{T_{ti}}\Delta P_{mi} + \frac{1}{T_{ti}}\Delta P_{gi} \\ \Delta\dot{P}_{gi} = -\frac{1}{T_{gi}}\Delta P_{gi} + \frac{1}{T_{gi}}\left(\Delta P_{ci} - \frac{1}{R_i}\Delta f\right) \end{cases}$$

By letting $x = (\Delta P_{g1}, \Delta P_{g2}, \Delta P_{m1}, \Delta P_{m2}, \Delta f)^T$, $\Delta P_c = (\Delta P_{c1}, \Delta P_{c2})^T$, then the following state-space model can be obtained:

$$\begin{cases} \dot{x}(t) = Ax(t) + B\Delta P_c(t) + E\Delta P_L, \\ \Delta f(t) = Cx(t), \end{cases} \tag{12}$$

where coefficient matrices A, B, E, and C are omitted here due to space limitation.

Since the objective of DSC is to drive the mismatched power to the operating interval of the online AGC units, then the power system (12) is stable by the PI control. That is, the remanding mismatched power can be accomplished by the AGC units finally in the steady-state.

In this test case, the load disturbance is assumed to be a step disturbance at $t = 50s$ with $\Delta P_L = 150MW$ ($\Delta P_L = 0.15$ per unit (pu), where the baseline power is $P_{base} = 1000MW$ and $\Delta P_{max}^{+} = 0.06$ pu). If all load aggregators do not participate in the frequency regulation, then the load disturbance is undertaken by the primary/supplementary control of generators. Obviously, additional spinning reserve capacity is needed for a large load disturbance, and the reserve capacity can be provided by both generating units and load agents.

In the following, we consider the DSC of multiple aggregated responsive loads. Suppose there are ten load aggregators under the bus agent with the maximal available regulation capacity of each aggregator given in the Tab. II.

TABLE II
MAXIMAL REGULATION CAPACITIES OF LOAD AGGREGATORS.

$P_{1,max}^L$ 16 MW	$P_{2,max}^L$ 12 MW	$P_{3,max}^L$ 24 MW	$P_{4,max}^L$ 12 MW	$P_{5,max}^L$ 40 MW
$P_{6,max}^L$ 28 MW	$P_{7,max}^L$ 10 MW	$P_{8,max}^L$ 8 MW	$P_{9,max}^L$ 30 MW	$P_{10,max}^L$ 20 MW

The total regulation capacity is $\sum_{j=1}^{10} P_{j,max}^L = 200MW$, i.e., $\sum_{j=1}^{10} P_{j,max}^L = 0.2$ pu. The communication structure among ten load aggregators and the pinning selection are given in Fig. 5, where only the first load aggregator is pinned. That is, the objective information is only shared with the first load aggregator, and the rest aggregators communicate with their neighbors.

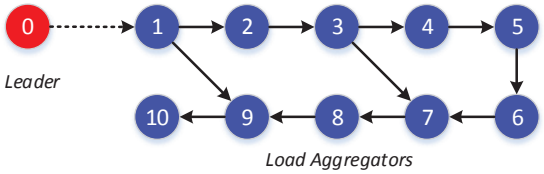

Fig. 5. The communication topology of ten load aggregators.

On the other hand, the plant disturbance $\omega(t) = [-0.04, \ldots, -0.02]^T w(t)$, where $w(t)$ is assumed to be an energy-limited Gaussian white noise (given in Fig. 6). The H_∞ performance index γ is chosen as 0.1 and the coefficient of AGC capacity is $\theta = 0.9$. By Algorithm 1 and pinning the first load aggregator, one can derive $\Theta = \{0.7723, \ldots, 0.5162\}$. The feedback gains κ and β are determined with $\kappa = 0.0296$, $\beta = 211.0856$. By simulation, one can find the convergence of the pinning equilibrium $\mu^* \approx 0.4892$ and active power changes of the load aggregators under the distributed pinning communication protocol (see Fig. 7) with the initial value of each load aggregator equal to its maximum available regulation capacity.

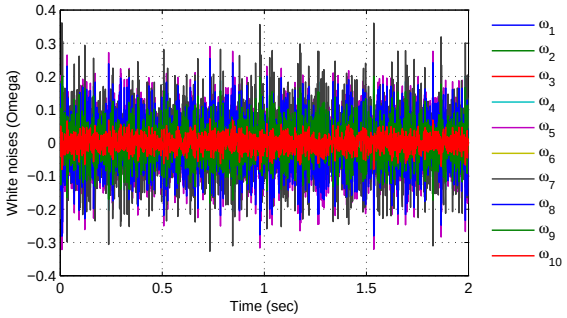

Fig. 6. The energy bounded white noise $\omega(t) = [\omega_1(t), \ldots, \omega_{10}(t)]$.

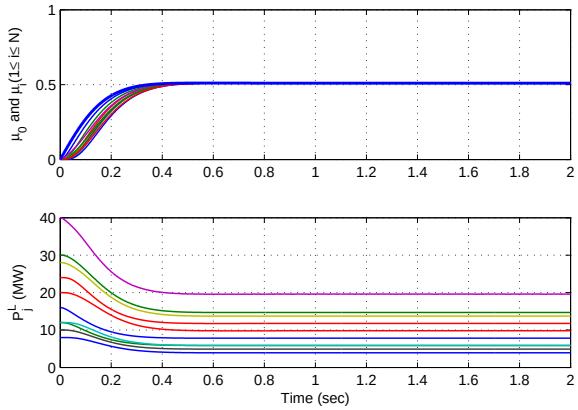

Fig. 7. The pinning equilibrium and pinning power changes of aggregated responsive loads.

As can be seen from Fig. 7, the optimal operation power $P_{j,*}^L$ for each load aggregator is $P_*^L = [8.3178, \ldots, 10.3992]$, and the curtailment for jth load aggregator is $\Delta P_j^L = P_{j,max}^L - P_{j,*}^L$. It is not difficult to calculate the total curtailment of load achieved by DSC is $\sum_{j=1}^{10} \Delta P_j^L = 95.9941$ MW. The pinning consensus trajectories can converge to the equilibrium within 2 seconds. If the load aggregators respond without time delays, then the dynamic response of frequency deviation and supplementary control output with and without demand side control are given in Fig. 8.

If load aggregators response with 3s time delay, then the dynamic response of frequency deviation and supplementary control output with and without load control are given in Fig. 9.

In fact, some load aggregators may respond with a longer time delay more than 3s with uncertainties. Thus, the expected

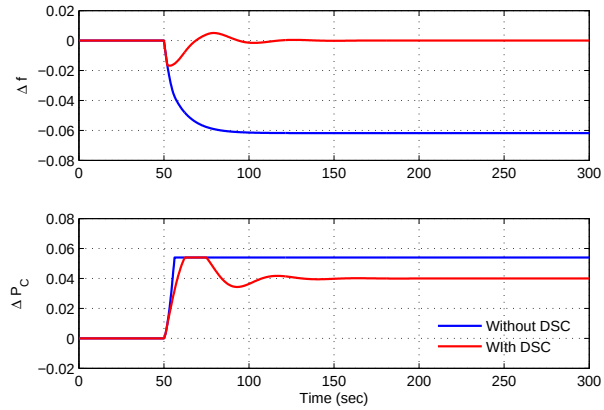

Fig. 8. Frequency deviation and control action for AGC units with/without DSC.

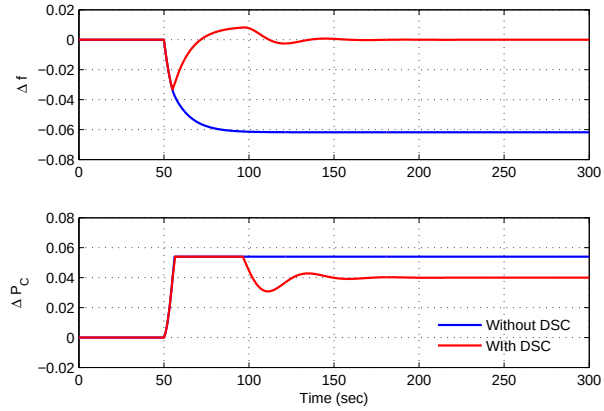

Fig. 9. Frequency deviation and control action for AGC units with/without DSC (3s response time delay for DSC).

active power regulation cannot be finished at one time in practice. Instead, the distributed pinning cooperative can be performed at each sampling instant with a sampling period (such as $\Delta t = 5$min). The main purpose of the proposed distributed strategy is to regulate the aggregated behavior of all responsive loads and make them participate in frequency control of the system under a large load disturbance, especially in the peak period of the power system.

In order to illustrate the communication delay on the stability of the proposed distributed protocol, we simulate the time-delayed case to show the robustness of the protocol to the small violations (time delays resulted from the communication network). Fig. 10 provides the simulation results, i.e., the changing of the pinning equilibrium and pinning power of the aggregators under two iteration cycles' delay for the distributed calculation. As can be seen from Fig. 10, the convergence of the distributed algorithm affected by small violations of the communication delay is acceptable.

B. Case 2: Time-varying communication topology

In this subsection, we intend to illustrate the effect of the communication failures to the performance of the distributed protocol in the demand side. The single-control area power

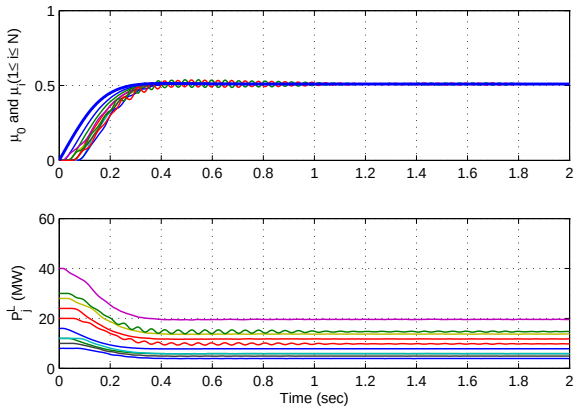

Fig. 10. The pinning equilibrium and pinning power changes of aggregated responsive loads with two iteration cycles' delay.

system model in Case 1 is still utilized to test the simulation. The main difference lies in that there are 200 load aggregators, which are placed and connected using an undirected scale-free network (the topology is omitted here for the space limit) instead of 10 load aggregators in Fig. 5; the step load disturbance occurs at two times and the communication topologies are time-varying ones. The load disturbance is assumed to be two step disturbances: at $t = 50s$ with $\Delta P_{L1} = 200MW$ ($\Delta P_{L1} = 0.2$ per unit (pu)), at $t = 350s$ with $\Delta P_{L2} = 150MW$ ($\Delta P_{L2} = 0.15$ pu) and the last five load aggregators dropped out from the communication network, which resulted in the communication network to be a piece-wise one. In this case study, we let the maximal regulation capacity of jth load aggregator $P^L_{j,max}$ to be a positive random number picked from the interval $[1, 3]$ and choose $\sum_{j=1}^{200} P^L_{j,max} = 400MW$ and the maximum regulation capacity for online AGC units is $\Delta P^+_{max} = 100MW$. The simulation results show that the proposed DSC algorithm is robust to communication failures and can realize the plug-in and plug-out of load aggregators.

Remark 4. *Scale-free network was first introduced in [31], in which the authors had found that a class of network exhibits a power-law degree distribution, at least asymptotically. That is, the fraction $P(k)$ of nodes in the network having k connections to other nodes goes for large k as $P(k) \sim k^{-\tilde{\gamma}}$, where $\tilde{\gamma}$ is a parameter whose value is typically in the range of $2 \sim 3$. Many networks have been reported to be scale-free, such as internet, the citation network, double-star electric power system dispatching data network, and power telecommunication network [32].*

Similar to the discussion about the stability of the primary and supplement control for generating units in Case 1, the joint control structure is stable since the objective of DSC is to drive the mismatched power to the operating interval of the online AGC units. And the remanding mismatched power can be accomplished by AGC units finally in the steady-state.

In the following, the external disturbance ω is still assumed to be an energy-limited white noise as in Case 1. The H_∞ performance index γ is chosen as 0.1 and the coefficients of

AGC capacity are $\theta_1 = 0.6$ and $\theta_2 = 0.9$. By Algorithm 1 and pinning 9 nodes according to maximum degree (i.e., nodes 1,3,4,5,6,9,17,20,83), one can derive the corresponding matrix Θ, which is omitted here. The feedback gains κ and β are given with $\kappa = 0.0112$, $\beta = 56.2164$. By simulation, one can derive the convergence of the first pinning equilibrium $\mu^* \approx 0.3499$ and the second pinning equilibrium $\mu^* \approx 0.7885$ and active power changes of the partial load aggregators under the distributed pinning communication protocol (see Fig. 11) with the initial value of each load aggregator is equal to its maximum available regulation capacity.

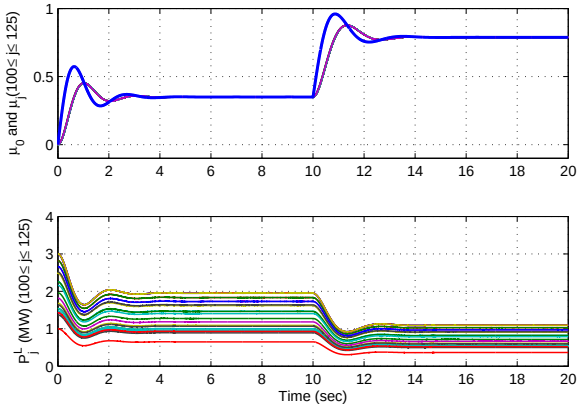

Fig. 11. The pinning equilibrium and pinning power changes of aggregated responsive loads.

As can be seen from Fig. 11, the expected mismatch power is shared by multiple load aggregators through communication network. The pinning consensus trajectories can converge to the first equilibrium within 4 seconds and to the second equilibrium within 4 seconds. The optimal operation power $P^L_{j,*}$ for each load aggregator after the first load disturbance is $P^L_* = [1.4626, \ldots, 1.2995]$, and the curtailment for jth load aggregator is $\Delta P^L_j = P^L_{j,max} - P^L_{j,*}$. It is easy to calculate the total curtailment of load achieved by DSC is $\sum_{j=1}^{200} \Delta P^L_j = 139.9986MW$. Similarly, one can derive the optimal operation power $P^L_{j,*}$ for each load aggregator after the second load disturbance is $P^L_* = [0.8213, \ldots, 0.7300]$, and the total curtailment of load achieved by DSC is $\sum_{j=1}^{195} \Delta P^L_j = 113.9942MW$.

Remark 5. *As for the changing of active power in Fig.11, the transient process of the convergence for the distributed pinning consensus algorithm experiences rebound and fluctuation, which are mainly caused by the communication network. Different communication structures contribute to different convergence rates and response time. While, the change of the regulation rate reflects the change of active power for the load aggregator which is an agglomeration effect. In practice, only the steady-state values of regulation rates are utilized for each load aggregator.*

If the load aggregators respond without time delays, then the dynamic response of frequency deviation and supplementary control output with and without demand side control are given in Fig. 12.

If the load aggregators respond with 3s time delay, then the dynamic response of frequency deviation and supplementary control output with and without demand side control are given in Fig. 13.

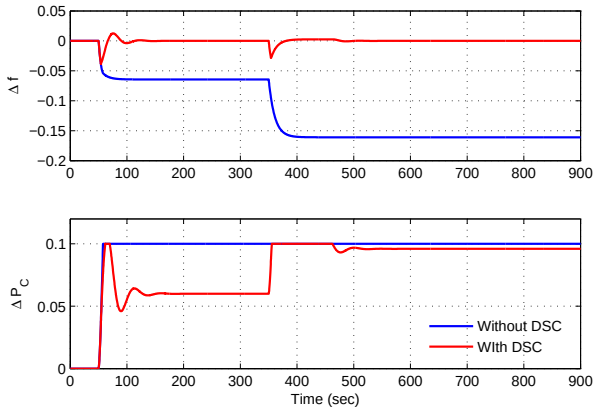

Fig. 12. Frequency deviation and control action for AGC units with/without DSC.

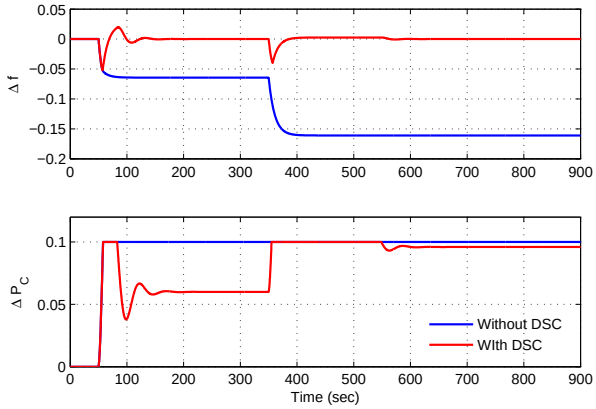

Fig. 13. Frequency deviation and control action for AGC units with/without DSC (3s response time delay for DSC).

As for the case of 3 seconds' time delays, the frequency with DSC will drop more than the free of time delay case, and the AGC units will sustain the power output for coupled of ten seconds until the load curtailment is achieved after 3 seconds' delay. In fact, there is an upper bound for the time delay of DSC and once the time delay has passed the upper bound, the frequency stability of the coupled control structure cannot be guaranteed until other spinning reserves are provided. As for the boundedness of PI controller output, it is because we assume that the capacity of AGC units is limited in each control area. The control action for AGC units cannot exceed its maximal regulation capacity, so the control action, i.e. ΔP_C, for the generating units is bounded. Under such a condition, frequency stability cannot be ensured without additional spinning reserves.

If all aggregated responsive loads do not participate in frequency regulation, then the load disturbance is undertaken by the primary/supplementary control of online AGC units with rate and capacity constraints, which are incapable of frequency regulation. Thus, additional spinning reserves are needed to

provide supplementary services; and load aggregators can be stimulated to reduce the consumption of active power for frequency regulation. The proposed distributed pinning control is able to coordinate these load aggregators to fulfill the expected regulation objective; and such a leader-following regulation process can be performed at multiple sampling instants until the frequency regulation capacity is derived to the regulation interval of online AGC units.

C. Case 3: Multi-control area power system

In this subsection, we consider the frequency stability problem of a three-control area power system, which is shown in Fig. 14. It is assumed that each control area has three generating units (part of them are AGC units) and lots of load aggregators which can provide supplementary frequency regulation services. The frequency control structure coupled by AGC and DSC has been provided in Fig. 2. For the generating units, all AGC units are controlled in a centralized PI controller with corresponding participation factors; For the load aggregators, they are controlled by the proposed distributed pinning control algorithm.

The DSC algorithm can achieve the fair participation for the load aggregators against the external disturbance based on the theoretical analysis in Theorem 1 and the PI control algorithm can regulate the active power output of AGC units with approximate feedback gains, which can ensure the coupled system (1) is stable. Both AGC units and load aggregators are cooperated to track the load disturbance and maintain the frequency stability.

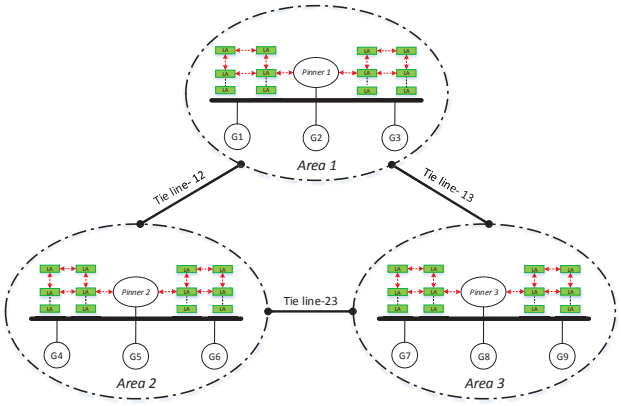

Fig. 14. Three-control area power system with multiple load aggregators in each area.

Next, we test the coupled control structure to verify the effectiveness of the demand side control algorithm. The power system parameters are given in Tab. III. While for the responsive loads, suppose there are 10, 15 and 12 load aggregators (they are connected using an undirected scale-free network) in control area $Ar1$, $Ar2$ and $Ar3$, respectively. The load disturbance is assumed to be a step disturbance in each control area: at $t = 100s$ with $\Delta P_{L1} = 100MW$, at $t = 300s$ with $\Delta P_{L2} = 150MW$, and at $t = 600s$ with $\Delta P_{L2} = 120MW$. The maximal regulation capacity of jth load aggregator in ith control area $P_{j,max}^{L,i}$ is a positive random number picked from the interval $[8, 12]$ and satisfies the $\sum_{j=1}^{10} P_{j,max}^{L,1} = 100MW$, $\sum_{j=1}^{15} P_{j,max}^{L,2} = 150MW$ and $\sum_{j=1}^{12} P_{j,max}^{L,3} = 120MW$; and online AGC units' capacities in each control area are $\Delta P_{max,1}^{+} = 100MW$, $\Delta P_{max,2}^{+} = 120MW$ and $\Delta P_{max,3}^{+} = 150MW$.

TABLE III
PARAMETERS USED FOR THE THREE-CONTROL AREA POWER SYSTEM.

Gen.	Rating(MW)	α_i	R_i(Hz/pu)	T_{gi}(s)	T_{ti}(s)
G1	1000	0.4	3.0	0.08	0.4
G2	800	0.4	3.0	0.06	0.36
G3	1000	0.2	3.3	0.07	0.42
G4	1100	0.6	2.7273	0.06	0.44
G5	900	0	2.667	0.06	0.32
G6	1200	0.4	2.5	0.08	0.4
G7	850	0	2.8235	0.07	0.3
G8	1000	0.5	3.0	0.07	0.4
G9	1020	0.5	2.9412	0.08	0.41
Area	D_i(pu/Hz)	$2H_i$(pu s)	B_i(pu/Hz)	$K_i(s)(/s)$	
Ar1	0.0143	0.1677	0.3483	$-0.0121 - 0.0672$	
Ar2	0.0161	0.2017	0.4140	$-0.0223 - 0.0583$	
Ar3	0.0152	0.1874	0.3692	$-0.0673 - 0.0676$	
$T_{12} = 0.12$, $T_{23} = 0.15$, $T_{13} = 0.25$				$P_{base} = 1000$ MW	

The external disturbance ω is still assumed to be an energy-limited white noise similar to the above two cases. The H_∞ performance index γ is chosen as 0.1 and the coefficients of AGC capacity are $\theta_{Ar1} = 0.6$, $\theta_{Ar2} = 0.8$ and $\theta_{Ar3} = 0.5$. By Algorithm 1 and pinning the first load aggregator in each control area, one can derive the corresponding matrix Θ_i, which is omitted here. The feedback gains κ_i and β_i can be derived from Algorithm 1 as well, which are given with $\kappa_1 = 0.0695$, $\beta_1 = 43.1532$, $\kappa_2 = 0.0549$, $\beta_2 = 53.8412$, $\kappa_3 = 0.0991$, $\beta_3 = 38.3732$. By simulation, one can derive the convergence of the pinning equilibrium and the corresponding active power changes for the aggregated responsive loads in each control area, which are given in Figs. 15-17.

Under the above parameters' setting and considering frequency compensation actions in each control area, one can run the simulation easily. Here, the system frequency responses in each control area are shown in Fig. 18 and the ACE deviations in each control area are given in Fig. 19.

It can be seen from the simulation results, the system frequency is greatly improved by considering the distributed control of populations of responsive loads. The participation of these responsive loads can assist the AGC units to fulfill the frequency regulation and relieve a part of AGC burden on the traditional power plants.

V. DISCUSSIONS

For the communication topology among the load aggregators, it is required that the joint communication topology has a directed spanning tree according to Theorem 1. The communication topology in Fig. 5 is just one satisfying the constraint (directed spinning tree). In fact, any communication topologies satisfying this constraint can be utilized for the communication of load aggregators. Such a constraint can be used as a guidance for the planning of the communication topology in the practical engineering implementation.

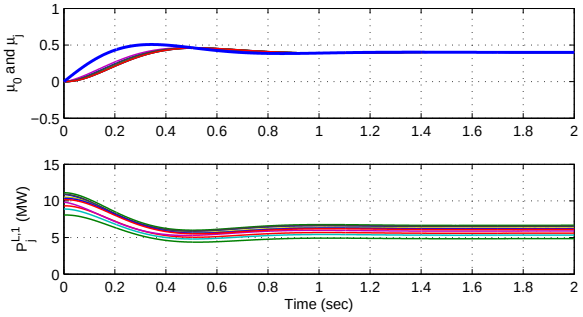

Fig. 15. The pinning equilibrium and pinning power changes of aggregated responsive loads in Area 1.

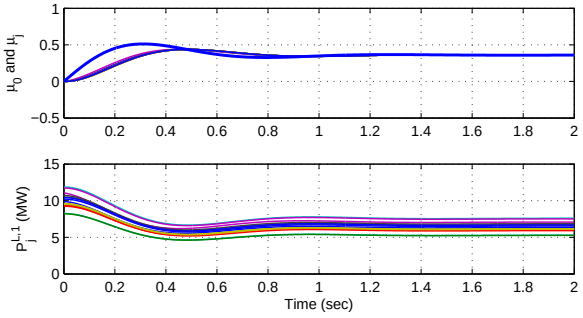

Fig. 16. The pinning equilibrium and pinning power changes of aggregated responsive loads in Area 2.

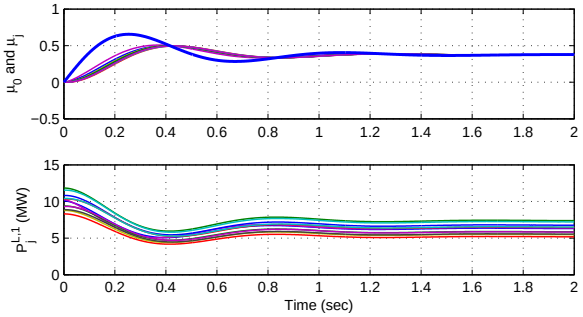

Fig. 17. The pinning equilibrium and pinning power changes of aggregated responsive loads in Area 3.

In an actual demand side control system, there are always two possibilities of time delays; one is the communication delay resulted from the communication network and another one is the responsive delay related to the dynamic response of the load aggregator. There is an upper bound for the time delay in the DSC; and once the time delay has passed the upper bound, the frequency stability of the coupled control structure cannot be guaranteed until other spinning reserves are provided. In our current work, we have simulated the communication delays to illustrate the robustness of the communication network and the responsive delay of load aggregator to show the relationship between the effective of the DSC and the supporting time of AGC units.

On the other hand, the maximal regulation capacity of each load aggregator is time-varying, which is not always available. We have illustrated this phenomenon in Case 2, where there are two load disturbances occurring at different time instants in this control area. The maximal regulation capacities of the

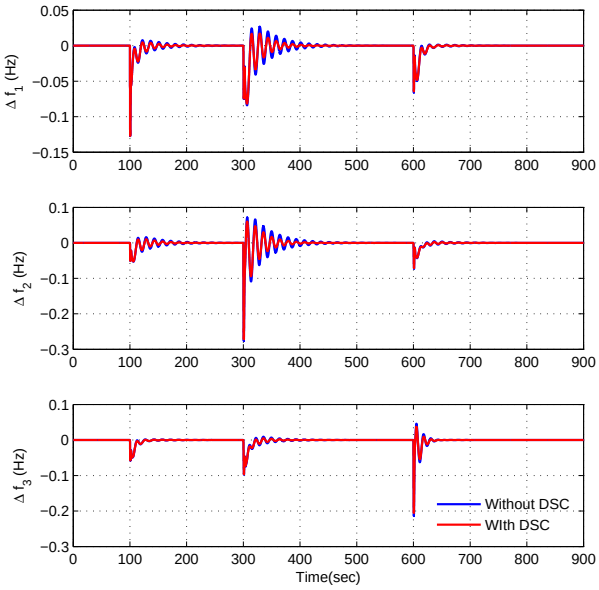

Fig. 18. Frequency deviations in three control areas with/without DSC.

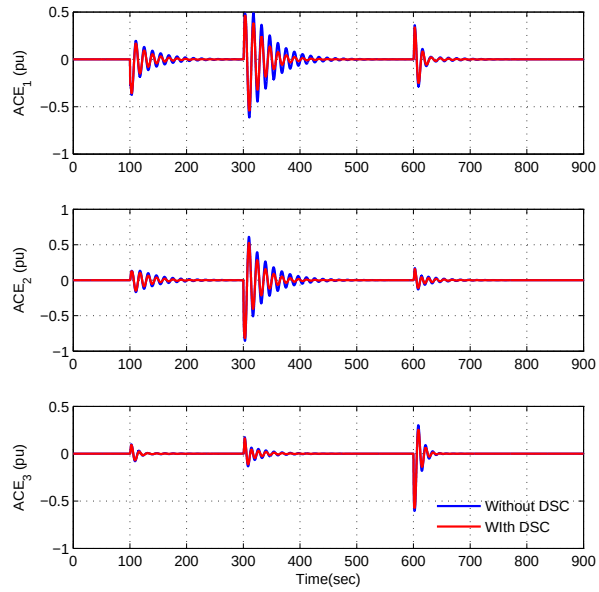

Fig. 19. ACE signals in three control areas with/without DSC.

load aggregators are reduced at the second load disturbance.

In the proposed demand side control algorithm, there are a centralized pinner and multiple load aggregators. For the pinner, independent system operator in each control area is responsible to initialize it and determine to send the objective information to which load aggregator. As for the load aggregator, it may be an energy management system for an intelligent residential district or a commercial building.

As for the coupled control structure (Fig. 2), the main challenge is that the load aggregator may not respond to the control input (utilization level for the load aggregator)

accurately due to the responsive uncertainties from load aggregators, which may result in the frequently action for the pinner. On the other hand, the load modeling is important to analyze the maximal capacity of an aggregator and to derive the approximate aggregated power of the load agent. In short, the participation of load aggregators is beneficial to the generating units since the load aggregators can provide faster reserve or regulation services without environmental contaminants. Meanwhile, such a DSC algorithm can improve the frequency stability by considering the primary and secondary regulation services provided by load aggregators.

VI. Conclusions

This paper presented a distributed pinning demand side control strategy for coordinating the operation of multiple load aggregators, which was integrated into the secondary frequency control of traditional power plants. Thus, a coupled frequency control structure by considering the traditional AGC and the proposed DSC was derived. For the distributed control of load aggregators, the convergence of the proposed distributed strategy was analyzed and the detailed designing steps were summarized as a multi-step algorithm for determining the feedback gains in the distributed pinning control. While, for the supplementary control of power plants, we still utilized the traditional centralized PI control to manage all AGC units in each control area. It was justified that the proposed coupled frequency framework can handle the plant disturbances for load aggregators and relieve the burden of traditional online AGC units. Furthermore, the system frequency could be improved by considering the AGC+DSC compared with AGC only.

Future works will explore the coordinating operation of multiple energy storage units [33]; centralized look-ahead dispatch for flexible load agents with responsive uncertainly [34] under the electricity market environment.

Appendix A
Proof of Theorem 1

Proof: Firstly, we study the stability of the error system (8) without disturbances. Consider the following Lyapunov candidate:

$$V(t)=\frac{1}{2}r^2(t)+\frac{1}{2}e^T(t)\Theta e(t), \tag{13}$$

where Θ is a positive definite matrix. Then the time derivative of $V(t)$ along the solution of error system (8) is

$$\begin{aligned}\dot{V}(t)=&-\kappa r(t)\big(B\mathbf{1}_N\big)r(t)-\kappa r(t)Be(t)\\&+\kappa r(t)\big(\Theta\mathbf{1}_NB\mathbf{1}_N\big)^Te(t)\\&-\beta e^T(t)\big(\Theta(L+D)+(L+D)^T\Theta\big)e(t)\\&+\kappa e^T(t)\big(\Theta\mathbf{1}_NB\big)e(t)\\\triangleq&z^T(t)\Omega z(t),\end{aligned}$$

where $z=[r^T(t),e^T(t)]^T$ and Ω is given as follows,

$$\Omega=\begin{bmatrix}-\kappa B\mathbf{1}_N & \frac{1}{2}\kappa\big((\Theta\mathbf{1}_NB\mathbf{1}_N)^T-B\big)\\ * & \kappa\Theta\mathbf{1}_NB-\beta[\Theta(L+D)+(L+D)^T\Theta]\end{bmatrix}.$$

By Schur complement Lemma, one knows that $\Omega<0$ is equivalent to $\kappa>0$ and

$$\begin{aligned}&\kappa\Theta\mathbf{1}_NB-\beta[\Theta(L+D)+(L+D)^T\Theta]\\&\quad+\frac{\kappa}{4B\mathbf{1}_N}[\Theta\mathbf{1}_NB\mathbf{1}_N-B^T][(\Theta\mathbf{1}_NB\mathbf{1}_N)^T-B]<0,\end{aligned}$$

that is,

$$\begin{aligned}\beta>&\frac{\kappa}{\lambda_{\min}}\Theta\mathbf{1}_NB+\frac{\kappa}{4\lambda_{\min}B\mathbf{1}_N}[\Theta\mathbf{1}_NB\mathbf{1}_N-B^T]\\&\times[(\Theta\mathbf{1}_NB\mathbf{1}_N)^T-B],\qquad(\kappa>0),\end{aligned}$$

where $\lambda_{\min}=\lambda_{\min}\big(\Theta(L+D)+(L+D)^T\Theta\big)$, which gives a discriminant relation for the feedback gains without disturbances.

Since condition (11) implies $\Omega<0$, the system (8) is asymptotically stable when disturbances $\omega_j(t)=0$, $j=1,\ldots,N$.

Subsequently, we discuss the performance of the system (8) with nonzero disturbance $\omega(t)$. Calculating the time derivative of $V(t)$ along the solution of (8) results in

$$\begin{aligned}\dot{V}(t)=&-\kappa r(t)\big(B\mathbf{1}_N\big)r(t)-\kappa r(t)Be(t)\\&+\kappa r(t)\big(\Theta\mathbf{1}_NB\mathbf{1}_N\big)^Te(t)\\&-\beta e^T(t)\big(\Theta(L+D)+(L+D)^T\Theta\big)e(t)\\&+\kappa e^T(t)\big(\Theta\mathbf{1}_NB\big)e(t)+e^T(t)\Theta\omega(t).\end{aligned}$$

For any $T>0$, consider the following cost function

$$J_T=\int_0^T[z^T(t)z(t)-\gamma^2\omega^T(t)\omega(t)]\mathrm{d}t.$$

According to the theory of linear systems [35], the solution of error system (8) is composed of two parts: one is the zero-input response associated with $\omega(t)\equiv\mathbf{0}$, which is independent on external disturbances; the other is the zero-state response under the initial state $z(t)\equiv\mathbf{0}$. Then, only the latter response related to the external disturbance $\omega(t)$ needs to be studied for the H_∞ performance of system (8), and thus, the initial state $z(0)$ is supposed to be zero-valued, i.e., $V(0)=0$. Under this initial condition, we have

$$\begin{aligned}J_T=&\int_0^T\big[z^T(t)z(t)-\gamma^2\omega^T(t)\omega(t)+\dot{V}(t)\big]\mathrm{d}t\\&-V(T)+V(0)\\=&\int_0^T\psi^T(t)\tilde{\Omega}\psi(t)\mathrm{d}t-V(T),\end{aligned}$$

where $\psi=[z^T(t),\omega^T(t)]^T$.

In terms of inequality (11) $\tilde{\Omega}<0$, which leads to $J_T<0$, i.e.,

$$\int_0^T\|z(t)\|^2\mathrm{d}t<\gamma^2\int_0^T\|\omega(t)\|^2\mathrm{d}t.$$

Let $T\to\infty$, one has $\int_0^\infty\|z(t)\|^2\mathrm{d}t<\gamma^2\int_0^\infty\|\omega(t)\|^2\mathrm{d}t$, which completes the proof. ■

Acknowledgements

The authors would like to give thanks to the anonymous reviewers and the handling editor for their valuable comments and suggestions, which had led to the improvement of the presentation and quality of this paper.

REFERENCES

[1] H. Bevrani, A. Ghosh, and G. Ledwich. Renewable energy sources and frequency regulation: survey and new perspectives. *IET Gener. Transm. Distrib.*, 4(5): 438–457, 2010.

[2] K. Dehghanpour and S. Afsharnia. Electrical demand side contribution to frequency control in power systems: a review on technical aspects. *Renew. Sust. Energ. Rev.*, 41: 1267–1276, 2015.

[3] F. Kennel, D. Gorges, and S. Liu. Energy management for smart grids with electric vehicles based on hierarchical MPC. *IEEE Trans. Ind. Informat.*, 9(3): 1528–1537, 2013.

[4] S. Weckx, R. Dhulst, and J. Driesen. Primary and secondary frequency support by a multi-agent demand control system. *IEEE Trans. Power Syst.*, 30(3): 1394–1404, 2014.

[5] J. Morren, S.W.H. de Haan, W.L. Kling, J.A. Ferreira. Wind turbines emulating inertia and supporting primary frequency control. *IEEE Trans. Power Syst.*, 21(1): 433–434, 2006.

[6] J.H. Chamberlin. C.W. Gellings. Demand-side management: concepts and methods. *US: The Fairmout Press Inc*, 1988.

[7] J.D. Kueck, A.F. Snyder, F. Li, and I.B. Snyder. Use of responsive load to supply ancillary services in the smart grid: Challenges and approach. *1st IEEE Int.Conf. Smart Grid Comm.*, Gaithersburg, MD, pp. 507–512, 2010.

[8] J. Aghaei and M.I. Alizadeh. Robust $n-k$ contingency constrained unit commitment with ancillary service demand response program. *IET Gener. Transm. Distrib.*, 8(12): 1928–1936, 2014.

[9] J. Wang, C.N. Bloyd, Z. Hu, and Z. Tan. Demand response in china. *Energy*, 35: 1592–1597, 2010.

[10] Assessment of demand response and advanced metering. *Federal Energy Regulatory Commission*, Report, 2008

[11] J. Aghaei and M.I. Alizadeh. Critical peak pricing with load control demand response program in unit commitment problem. *IET Gener. Transm. Distrib.*, 7(7): 681–690, 2013.

[12] H. Hao, B.M. Sanandaji, K. Poolla, and T.L. Vincent. Aggregate flexibility of thermostatically controlled loads. *IEEE Trans. Power Syst.*, 30(1): 189–198, 2015.

[13] D. Wang, S. Parkinson, W. Miao, H. Jia, C. Crawford, and N. Djilali. Hierarchical market integration of responsive loads as spinning reserve. *Appl. Energy*, 104: 229–238, 2013.

[14] L.R. Chang-Chien, L.N. An, T.W. Lin, and W.J. Lee. Incorporating demand response with spinning reserve to realize an adaptive frequency restoration plan for system contingencies. *IEEE Trans. Smart Grid*, 3(3): 1145–1153, 2012.

[15] N. Lu and Y. Zhang. Design considerations of a centralized load controller using thermostatically controlled appliances for continuous regulation reserves. *IEEE Trans. Smart Grid*, 4(2): 914–921, 2013.

[16] J.A. Short, D.G. Infield, and L.L. Freris. Stabilization of grid frequency through dynamic demand control. *IEEE Trans. Power Syst.*, 22(3): 1284–1293, 2007.

[17] A. Molina-García, F. Bouffard, and D.S. Kirschen. Decentralized demand-side contribution to primary frequency control. *IEEE Trans. Power Syst.*, 26(1): 411–419, 2011.

[18] C. Zhao, U. Topcu, and S.H. Low. Optimal load control via frequency measurement and neighborhood area communication. *IEEE Trans. Power Syst.*, 28(4): 3576–3587, 2013.

[19] B. Kirby, M. Starke, and S. Adhikari. Nyiso industrial load response opportunities: Resource and market assessment-Task 2 final report. *Oak Ridge National Laboratory, Oak Ridge, Tennessee*, 2009.

[20] Y. Xu, W. Liu, and J. Gong. Stable multi-agent-based load shedding algorithm for power systems. *IEEE Trans. Power Syst.*, 26(4): 2006–2014, 2011.

[21] G. Mokhtari, G. Nourbakhsh, and A. Ghosh. Smart coordination of energy storage units for voltage and loading management in distribution networks. *IEEE Trans. Power Syst.*, 28(4): 4812–4820, 2013.

[22] M.H. Nazari, Z. Costello, M.J. Feizollahi, S. Grijalva, and M. Egerstedt. Distributed frequency control of prosumer-based electric energy systems. *IEEE Trans. Power Syst.*, 29(6): 2934–2942, 2014.

[23] C. Chen, J. Wang, and S. Kishore. A distributed direct load control approach for large-scale residential demand response. *IEEE Trans. Power Syst.*, 29(5): 2219–2228, 2014.

[24] Q. Shafiee, J.M. Guerrero, and J.C. Vasquez. Distributed secondary control for islanded microgrids-A novel approach. *IEEE Trans. Power Electron.*, 29(2): 1018–1031, 2014.

[25] K. Zhou, J.C. Doyle, K. Glover, et al. Robust and optimal control. *Prentice Hall New Jersey*, 1996.

[26] J. Hu, J. Cao, J. Yu, and T. Hayat. Consensus of nonlinear multi-agent systems with observer-based protocols. *Systems Control Lett.*, 72: 71–79, 2014.

[27] Z. Li, G. Wen, Z. Duan, and W. Ren. Designing fully distributed consensus protocols for linear multi-agent systems with directed graphs. *IEEE Trans. Automat. Control*, 60(4): 1152–1157, 2015.

[28] H. Su, M.Z.Q. Chen, J. Lam, and Z. Lin. Semi-global leader-following consensus of linear multi-agent systems with input saturation via low gain feedback. *IEEE Trans. Circuits Syst. I, Reg. Papers*, 60(7): 1881–1889, 2013.

[29] J. Nutaro, and V. Protopopescu. The impact of market clearing time and price signal delay on the stability of electric power markets. *IEEE Trans. Power Syst.*, 24(3): 1337–1345, 2009.

[30] J.P. Hespanha, P. Naghshtabrizi, and Y. Xu. A survey of recent results in networked control systems. *Proc. IEEE*, 95(1): 138–162, 2007.

[31] A.L. Barabási and R. Albert. Emergence of scaling in random networks. *Science*, 286(5439): 509–512, 1999.

[32] J. Hu, J. Yu, J. Cao, M. Ni, and W. Yu. Topological interactive analysis of power system and its communication module: A complex network approach. *Physica A*, 416: 99–111, 2014.

[33] J. Aghaei and M. I. Alizadeh. Multi-objective self-scheduling of chp-based microgrids considering demand response programs and ESSs. *Energy*, 55: 1044–1054, 2013.

[34] C. Zhao, J. Wang, J.-P. Watson, and Y. Guan. Multi-stage robust unit commitment considering wind and demand response uncertainties. *IEEE Trans. Power Syst.*, 28(3): 2708–2717, 2013.

[35] C.-T. Chen. Linear system theory and design. *Oxford University Press, Inc.*, 1995.

Jianqiang Hu received the B.S. degree from the North China University of Water Resources and Electric Power, Zhengzhou, China, in 2010, and the M.S. degree from Southeast University, Nanjing, China, in 2013, where he is currently pursuing the Ph.D. degree with the School of Automation. His current research interests include synchronization of complex networks, cooperative control of multi-agent systems, power system stability and control, and demand-side distributed control.

Dr. Hu was a recipient of the Outstanding Masters Degree Thesis Award from Jiangsu Province, China, in 2014.

Jinde Cao (M'07-SM'07) received the B.S. degree from Anhui Normal University, Wuhu, China, in 1986, the M.S. degree from Yunnan University, Kunming, China, in 1989, and the Ph.D. degree from Sichuan University, Chengdu, China, in 1998, all in mathematics/applied mathematics.

He was with Yunnan University from 1989 to 2000, where he was a Professor from 1996 to 2000. In 2000, he joined the Department of Mathematics, Southeast University, Nanjing, China. From 2001 to 2002, he was a Post-Doctoral Research Fellow with the Department of Automation and Computer-Aided Engineering, Chinese University of Hong Kong, Hong Kong, and a Visiting Research Fellow and Visiting Professor with the School of Information Systems, Computing and Mathematics, Brunel University, Uxbridge, U.K., from 2006 to 2008. He is currently a Distinguished Professor and Doctoral Advisor with Southeast University, and also a Distinguished Adjunct Professor with King Abdulaziz University, Jeddah, Saudi Arabia. He has authored or co-authored over 300 journal papers and five edited books. His current research interests include nonlinear systems, neural networks, complex systems and complex networks, stability theory, and applied mathematics.

Dr. Cao was an Associate Editor of the IEEE TRANSACTIONS ON NEURAL NETWORKS, the Journal of the Franklin Institute, and Neurocomputing. He is an Associate Editor of the IEEE TRANSACTIONS ON CYBERNETICS, Differential Equations and Dynamical Systems, Mathematics and Computers in Simulation, and Neural Networks. He is a reviewer of Mathematical Reviews and Zentralblatt-Math. He was an ISI Highly-Cited Researcher in Mathematics and Engineering listed by Thomson Reuters.

Josep M. Guerrero (S'01-M'04-SM'08-F'15) received the B.S. degree in telecommunications engineering, the M.S. degree in electronics engineering, and the Ph.D. degree in power electronics from the Technical University of Catalonia, Barcelona, in 1997, 2000 and 2003, respectively. He was an Associate Professor with the Department of Automatic Control Systems and Computer Engineering, Technical University of Catalonia, teaching courses on digital signal processing, field-programmable gate arrays, microprocessors, and control of renewable energy. In 2004, he was responsible for the Renewable Energy Laboratory, Escola Industrial de Barcelona. Since 2011, he has been a Full Professor with the Department of Energy Technology, Aalborg University, Aalborg East, Denmark, where he is responsible for the microgrid research program. From 2012 he is also a guest Professor at the Chinese Academy of Science and the Nanjing University of Aeronautics and Astronautics, and since 2014, he has been a Chair Professor at Shandong University, Jinan, China. His research interests is oriented to different microgrid aspects, including power electronics, distributed energy-storage systems, hierarchical and cooperative control, energy management systems, and optimization of microgrids and islanded minigrids.

Prof. Guerrero was the recipient of the Highly Cited Researcher Award by Thomson Reuters in 2014. He is an Associate Editor of the IEEE TRANSACTIONS ON POWER ELECTRONICS, the IEEE TRANSACTIONS ON INDUSTRIAL ELECTRONICS, and the IEEE INDUSTRIAL ELECTRONICS MAGAZINE, and an Editor of the IEEE TRANSACTIONS ON SMART GRID. He was a Guest Editor of the IEEE TRANSACTIONS ON POWER ELECTRONICS Special Issue on Power Electronics for Wind Energy Conversion and Power Electronics for Microgrids; the IEEE TRANSACTIONS ON INDUSTRIAL ELECTRONICS Special Section on Uninterruptible Power Supplies Systems, Renewable Energy Systems, Distributed Generation, and Microgrids; and Industrial Applications, and Implementation Issues of the Kalman Filter; and the IEEE TRANSACTIONS ON SMART GRID Special Issue on Smart DC Distribution Systems. He was the Chair of the Renewable Energy Systems Technical Committee of the IEEE Industrial Electronics Society.

Taiyou Yong received the B.S. and M.S. degrees from Tsinghua University, Beijing, China in 1991 and 1995, respectively, and the Ph.D. degree from University of Wisconsin-Madison, USA in 2001. He had worked and consulted with ABB, California ISO and EPRI for more than 15 years. Currently he is with China Electric Power Research Institute. His research interests include electricity market operations, power system operations and renewable integration.

Jie Yu received her B.S. and M.S. in Electrical Engineering from Southeast University, China, at July 1996 and March 2000, respectively. She had been employed as power system monitoring software engineer in State Grid Electric Power Research Institute, Nanjing, from April 2000 to March 2006. And then, she pursued her Ph.D. in Electricity Engineering at Southeast University. In June 2009, she received her Ph.D and was engaged as associate professor in School of Electrical Engineering, Southeast University. She mainly majors in power optimization dispatch, renewable generation, and power system monitoring technology.